First-principles modeling of quantum nuclear effects and atomic interactions in solid ^{4}He at high pressure

Claudio Cazorla[1] and Jordi Boronat[2,*]

[1]*School of Materials Science and Engineering, University of New South Wales, Sydney NSW 2052, Australia*

[2]*Departament de Física i Enginyeria Nuclear, Universitat Politècnica de Catalunya, Campus Nord B4-B5, E-08034, Barcelona, Spain*

(Received 17 September 2014; published 7 January 2015)

We present a first-principles computational study of solid ^{4}He at $T = 0$ K and pressures up to ∼160 GPa. Our computational strategy consists in using van der Waals density functional theory (DFT-vdW) to describe the electronic degrees of freedom in this material, and the diffusion Monte Carlo (DMC) method to solve the Schrödinger equation describing the behavior of the quantum nuclei. For this, we construct an analytical interaction function based on the pairwise Aziz potential that closely matches the volume variation of the cohesive energy calculated with DFT-vdW in dense helium. Interestingly, we find that the kinetic energy of solid ^{4}He does not increase appreciably with compression for $P \geqslant 85$ GPa. Also, we show that the Lindemann ratio in dense solid ^{4}He amounts to 0.10 almost independently of pressure. The reliability of customary quasiharmonic DFT (QH DFT) approaches in describing quantum nuclear effects in solids is also studied. We find that QH DFT simulations, although provide a reasonable equation of state in agreement with experiments, are not able to reproduce correctly these critical effects in compressed ^{4}He. In particular, we disclose huge discrepancies of at least ∼50% in the calculated ^{4}He kinetic energies using both the QH DFT and present DFT-DMC methods.

DOI: 10.1103/PhysRevB.91.024103 PACS number(s): 67.80.−s, 02.70.Ss

I. INTRODUCTION

Solid helium typifies an extreme quantum condensed-matter system. Due to the light mass of the atoms and weak interparticle interactions, quantum nuclear delocalization effects become crucially important in this crystal. At absolute zero temperature, ^{4}He atoms move agitatedly around the equilibrium positions of their hexagonal closed packed (hcp) lattice, producing unusually large kinetic energies (that is, comparable in magnitude to the potential energy), and major anharmonic effects [1–3].

In order to fully understand and make quantitative predictions on the quantum nature of solid ^{4}He, it is necessary to solve the corresponding Schrödinger equation. This represents an extremely challenging mathematical problem due to the complexity of the calculations involved and large number of nuclear and electronic degrees of freedom to be considered. Fortunately, at normal conditions helium atoms are, from an electronic band-structure point of view, very elementary particles thereby the ^{4}He–^{4}He interactions can be effectively modeled with simple analytical expressions that exclusively depend on the interatomic distances (e.g., Lennard–Jones- and Aziz-like potentials) [4,5]. By making use of these simplifications and employing advanced quantum simulation methods (e.g., quantum Monte Carlo), it has been possible to determine with tremendous accuracy and computational efficiency the ground-state properties of solid ^{4}He [5,6]. The same kind of approach has been successfully applied also to the study of similar systems like H_2, LiH, LiD, and Ne [7–11].

A fundamental question that remains to be answered at the quantitative level is: how important quantum nuclear effects turn out to be in solid helium (and other quantum crystals) under increasing pressure? As compression is raised the repulsive electrostatic interactions between neighboring clouds of electrons increase and consequently the atoms remain closer to their equilibrium positions in order to minimize the potential energy, E_{pot}. By other side, due to the noncommutativity between the position and momentum quantum operators, whenever atomic localization increases so does the kinetic energy, E_{kin}. Namely, pressure acts by incrementing both E_{pot} and E_{kin} energies, and it is not explicitly known how the $|E_{\text{kin}}/E_{\text{pot}}|$ ratio, which can be regarded as a quantum level indicator of the system, evolves under compression. Answering to this and other similar questions is of paramount importance for modeling of materials in Earth and planetary sciences, since light weight species like ^{4}He and H_2 are believed to be abundant in the interior of celestial bodies. More precisely, determining the exact role of quantum nuclear effects in compressed quantum crystals will allow to justify or disapprove the use of approximate approaches, routinely employed in high-pressure studies (e.g., Debye and quasiharmonic models) [12–19], for estimation of "zero-point energies" and related quantities (e.g., phase transitions and atomic structure).

Quantifying the exact evolution of the energy in ^{4}He under pressure, however, is not a simple task. Since compression profoundly affects the electronic structure of materials, the interaction models which at low pressures describe successfully ^{4}He atoms or H_2 molecules turn out to be unreliable at high-P conditions. This fact seriously hinders the application of quantum Monte Carlo methods to their study. From an ideal point of view, one would like to describe both the electronic and nuclear degrees of freedom in quantum crystals fully from first principles, that is, without relying on any substantial approximation to the atomic interactions. Nevertheless, such a strategy, although in principle is technically possible, it would require of an enormous amount of computational effort. Thus, in practice, effective and simpler quantum simulation methods able to deal with large systems (i.e., composed of 100–1000 atoms) are highly desirable.

*ccazorla@icmab.es

In this work, we present a comprehensive computational study of the energy and structural properties of hcp ^{4}He at $T = 0$ K and pressures up to ∼160 GPa, based exclusively on first-principles methods. In particular, we employ density functional theory (DFT) to access the electronic band structure of the crystal and the diffusion Monte Carlo (DMC) method to solve the time-dependent Schrödinger equation governing the behavior of the quantum nuclei. The effective pair interaction between nuclei is constructed by fitting the static compression curve obtained with DFT to an analytical function based on the Aziz potential [4] and an attenuation repulsion factor proposed by Moraldi [20]. We find that the $|E_{\rm kin}/E_{\rm pot}|$ ratio in solid ^{4}He is overall depleted with increasing pressure due to very small (large) increase of $E_{\rm kin}$ ($E_{\rm pot}$) at compressions larger than ∼85 GPa. In particular, the ^{4}He kinetic energy increases by no more than ∼15 K in the pressure interval $85 \leqslant P \leqslant 150$ GPa. Such a small $E_{\rm kin}$ increase illustrates the unique ability of ^{4}He atoms to remain extraordinarily delocalized within extremely dense environments as a result of quantum correlations. Accordingly, we find that the Lindenmann ratio in compressed ^{4}He ($P \geqslant 15$ GPa) amount to 0.10 almost independently of the pressure. Furthermore, we assess the performance of approximate quasiharmonic DFT methods in evaluation of kinetic energies at $T = 0$ K and find that, in the best of the cases, these approaches exceedingly overestimate $E_{\rm kin}$ by ∼50%. Quasiharmonic approaches also turn out to be inadequate in describing the size of the ^{4}He displacements around their equilibrium lattice positions. Thus we resolve that quasiharmonic DFT methods are not able to describe the ground-state properties of dense helium correctly. The main conclusions presented in this work can be extended to other light and weakly interacting species like, for instance, H_2, methane (CH_4), and ammonia (NH_3), wherein quantum nuclear effects are expected to be also critically important [21–25].

The organization of this article is as follows. In the next section, we briefly explain the fundamentals of the methods employed and provide the technical details in our calculations. There, we present also our modeling strategy of the atomic interactions in solid ^{4}He at high P. Next, we present our results for the equation of state, $|E_{\rm kin}/E_{\rm pot}|$ ratio, and structural properties of solid helium, together with some discussion. Finally, we summarize our main findings in Sec. IV.

II. COMPUTATIONAL METHODS

In this work, density functional theory (DFT) provides the basis for our understanding of the electronic structure of solid ^{4}He under pressure. In particular, we use the DFT output to construct an effective pairwise potential that makes it possible to simulate quantum helium crystals with the diffusion Monte Carlo (DMC) method at low computational cost. In the next subsections, we briefly explain the basics of the DFT and DMC methods and present our proposed and easy-to-implement parametrization of the ^{4}He–^{4}He interactions at high pressures (i.e., up to ∼160 GPa). Also we review the main ideas of the quasiharmonic approach, which is customarily employed for the estimation of zero-temperature kinetic energies in computational high-P studies.

A. Density functional theory

DFT is a first-principles approach, which has allowed for accurate and reliable knowledge of a great deal of materials with exceptional computational affordability [26,27]. There is only one uncontrollable approximation in DFT, namely, the functional used for the exchange-correlation energy $E_{\rm xc}$. There is abundant evidence showing that commonly used $E_{\rm xc}$ functionals yield accurate results for a range of properties of metallic and nonmetallic crystals, including the equilibrium lattice parameter, elastic constants, phonon frequencies, $T = 0$ equation of state (EOS) and solid-state phase boundaries [28–30].

It must be noted, however, that standard DFT methods do not describe properly long-range dispersive interactions in solids, like for instance van der Waals (vdW) forces, due to the local nature of the employed $E_{\rm xc}$ approximations [31,32]. Also, it is well-known that such a type of interactions plays a critical role in the cohesion of helium at low pressures. Nevertheless, short-range effects in rare-gas systems become increasingly more relevant as pressure is raised. Consequently, the description of helium and other similar materials attained with standard DFT becomes progressively more accurate as density is increased [33,34]. In spite of this fact, we explicitly treat dispersive interactions in this work by employing Grimme's vdW approach [36] and the exchange-correlation functional due to Perdew *et al.* [35] (hereafter denoted as PBE-vdW). As it will be shown later, considering long-range vdW interactions in our calculations has imperceptible effects on the final conclusions.

A completely separate issue from the choice of $E_{\rm xc}$ is the implementation of DFT, which mainly concerns to the way in which electron orbitals are represented. Here, we have chosen the PAW ansatz [37,38] as implemented in the VASP code [39] since it has been demonstrated to be greatly efficient [40,41]. Regarding other technical aspects in our DFT calculations, the electronic wave functions were represented in a plane-wave basis truncated at 500 eV, and for integrations within the first Brillouin zone (BZ) we employed dense Γ-centered k-point grids of 14×14×14. By using these parameters we obtained interaction energies that were converged to within 5 K per atom. Geometry relaxations were performed by using a conjugate-gradient algorithm that kept the volume of the unit cell fixed while permitting variations of its shape, and the imposed tolerance on the atomic forces was 0.005 eV Å^{-1}. With this DFT setup, we calculated the total energy of solid ^{4}He in the volume interval $3 \leqslant V \leqslant 16$ Å^3/atom.

B. Zero-point energy within the quasiharmonic approach

In the quasiharmonic (QH) approach, one assumes that the potential energy of a crystal can be approximated with a quadratic expansion around the equilibrium atomic configuration of the form

$$E_{\rm harm} = E_{\rm eq} + \frac{1}{2} \sum_{l\kappa\alpha, l'\kappa'\alpha'} \Phi_{l\kappa\alpha, l'\kappa'\alpha'} u_{l\kappa\alpha} u_{l'\kappa'\alpha'}, \qquad (1)$$

where $E_{\rm eq}$ is the total energy of the undistorted lattice, $\mathbf{\Phi}$ the force-constant matrix, and $u_{l\kappa\alpha}$ is the displacement along Cartesian direction α of the atom κ at lattice site l. Usually,

the associated dynamical problem is tackled by introducing

$$u_{l\kappa\alpha}(t) = \sum_q u_{q\kappa\alpha} \exp\left[i\left(\omega t - \boldsymbol{q}\cdot(\boldsymbol{l}+\boldsymbol{\tau}_\kappa)\right)\right], \quad (2)$$

where $\boldsymbol{q}$ is a wave vector in the first Brillouin zone (BZ) defined by the equilibrium unit cell; $\boldsymbol{l}+\boldsymbol{\tau}_\kappa$ is the vector that locates the atom κ at cell l in the equilibrium structure. Then, the normal modes are found by diagonalizing the dynamical matrix

$$D_{\boldsymbol{q};\kappa\alpha,\kappa'\alpha'} = \frac{1}{\sqrt{m_\kappa m_{\kappa'}}} \sum_{l'} \Phi_{0\kappa\alpha,l'\kappa'\alpha'} \exp\left[i\boldsymbol{q}\cdot(\boldsymbol{\tau}_\kappa - \boldsymbol{l}' - \boldsymbol{\tau}_{\kappa'})\right], \quad (3)$$

and thus the material is treated as a collection of noninteracting harmonic oscillators with frequencies $\omega_{\boldsymbol{q}s}$ (positively defined and nonzero) and energy levels

$$E^n_{\boldsymbol{q}s} = \left(\tfrac{1}{2}+n\right)\omega_{\boldsymbol{q}s}, \quad (4)$$

where $0 \leqslant n < \infty$. Within this approximation, the Helmholtz free energy of a crystal with volume V at temperature T is given by

$$F_{\rm harm}(V,T) = \frac{1}{N_q} k_B T \sum_{\mathbf{q}s} \ln\left[2\sinh\left(\frac{\hbar\omega_{\mathbf{q}s}(V)}{2k_{\rm B}T}\right)\right], \quad (5)$$

where N_q is the total number of wave vectors used in the BZ integration, and the explicit V dependence of the frequencies is indicated. In the limit of zero-temperature, Eq. (5) transforms into

$$E_{\rm harm}(V) = \frac{1}{N_{\rm q}} \sum_{\boldsymbol{q}s} \frac{1}{2}\hbar\omega_{\boldsymbol{q}s}(V), \quad (6)$$

which usually is referred to as the "zero-point energy" (ZPE). We note that in many computational high-P studies ZPE corrections turn out to be decisive in the prediction of accurate transition pressures, which involve two crystal structures with similar $E_{\rm eq}$ energies [12,13,42].

In order to compute the QH free energy of a crystal, it is necessary to know its full phonon spectrum. For this, we employ here the "direct approach" and DFT calculations. In the direct approach, the force-constant matrix is directly calculated in real-space by considering the proportionality between the atomic displacements and forces when the former are sufficiently small [43,44]. In this case, large supercells have to be constructed in order to guarantee that the elements of the force-constant matrix have all fallen off to negligible values at their boundaries, a condition that follows from the use of periodic boundary conditions [45]. Once the force-constant matrix is obtained, we can Fourier-transform it to obtain the phonon spectrum at any q point.

The quantities with respect to which our QH DFT calculations need to be converged are the size of the supercell, the size of the atomic displacements, and the numerical accuracy in the calculation of the atomic forces and BZ sampling. We found the following settings to fulfill convergence of ZPE corrections to within 5 K/atom: 4×4×3 supercells (i.e., 48 repetitions of the hcp unit cell containing a total of 96 atoms), atomic displacements of 0.02 Å, and special Monkhorst-Pack [46] grids of 12×12×12 q points to compute the sums in Eq. (5). Regarding the calculation of the atomic forces with VASP, we found that the density of k points had to be increased slightly with respect to the value used in the energy calculations (i.e., from 14×14×14 to 16×16×16) and that computation of the nonlocal parts of the pseudopotential contributions had to be performed in reciprocal, rather than real, space. These technicalities were adopted in all our force-constant matrix calculations. The value of the phonon frequencies and ZPE energies were obtained with the PHON code due to Alfè [45]. In using this code, we exploited the translational invariance of the system to impose the three acoustic branches to be exactly zero at the Γ q point, and used central differences in the atomic forces (i.e., we considered positive and negative atomic displacements). As an example of our phonon frequency calculations, we show in Fig. 1 the full ^{4}He phonon spectrum computed at $P \sim 40$ GPa. It is noted that the effect of considering van der Waals forces there is remarkably small.

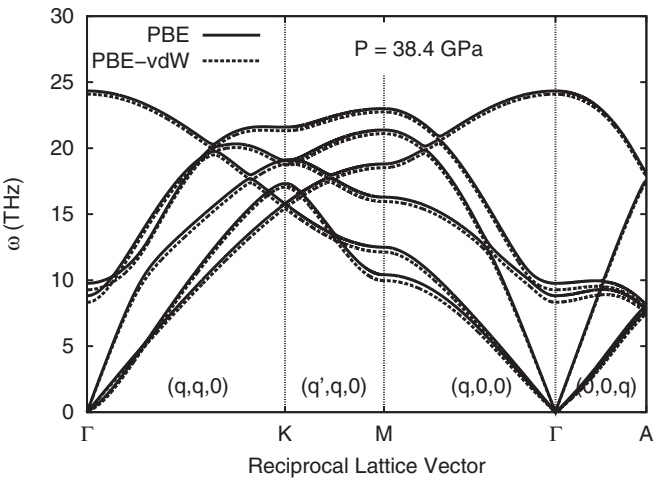

FIG. 1. Phonon spectrum of solid ^{4}He calculated at high pressure with DFT using two different exchange-correlation energy functionals, one of which takes into account long-range attractive van der Waals interactions (see text).

C. Construction of the effective interatomic potential $V_{\rm Aziz\text{-}B}$

In a previous work, we demonstrated that the semiempirical pairwise potential due to Aziz [4] is not appropriate to describe solid ^{4}He at pressures higher than ∼1 GPa [28]. The Aziz potential, $V_{\rm Aziz}(r)$ (where r represents the radial distance between a pair of atoms), is composed of two basic contributions: (1) $V_{\rm rep}(r)$, which is short-ranged and repulsive and accounts for the electrostatic and Pauli-like interactions between close electrons, and (2) $V_{\rm bond}(r)$, which is long-ranged and attractive and describes the interactions between instantaneous and induced multipoles created in the electron clouds. As pressure is raised, electronic repulsion prevails over attraction, namely $V_{\rm rep} \gg V_{\rm bond}$. In the Aziz case, however, we found that $V_{\rm rep}$ is unrealistically too large at small r. In order to ammend this flaw, we performed a series of DFT (PBE-vdW) energy calculations considering different configurations in which ^{4}He atoms were fixed on their equilibrium hcp positions. Subsequently, we fitted a modified version of the Aziz potential, hereafter denoted as $V_{\rm Aziz\text{-}M}(r)$, to our DFT (PBE-vdW) results. The form of this modified Aziz

potential is based on the model proposed by Moraldi for solid H_2 [20], which reads

$$V_{\text{Aziz-M}}(r) = V_{\text{rep}}(r)\, f_{\text{att}}(r) + V_{\text{bond}}(r). \tag{7}$$

In the above equation, V_{rep} and V_{bond} are the original repulsive and attractive parts found in the Aziz potential, respectively, and f_{att} is an attenuation repulsion factor of the form

$$f_{\text{att}}(r) = \begin{cases} \exp\left[-A_{\text{att}}\left(\dfrac{R_{\text{att}}}{r} - 1\right)^{C_{\text{att}}}\right] & r \leqslant R_{\text{att}}, \\ 1 & r > R_{\text{att}}, \end{cases} \tag{8}$$

where A_{att}, R_{att}, and C_{att} are parameters to be determined.

In our fitting strategy, rather than trying to match the set of calculated DFT energies, we pursued to reproduce the static DFT equation of state [i.e., $P_{\text{static}} = -dE_{\text{DFT}}(V)/dV$]. In fact, the physics contained in any pair of potential functions $V_2(r)$ and $V_2'(r) = V_2(r) + V_0$ (where V_0 is a constant) is the same, hence the truly important quantities to reproduce are variations of the total energy with respect to the atomic positions (e.g., pressure and atomic forces). For this, we fitted the DFT energies to a third order Birch-Murnaghan equation of the form [47]

$$\begin{aligned} E_{\text{eq}}(V) = {} & E_0 + \frac{3}{2}V_0 B_0 \\ & \times \left[-\frac{\chi}{2}\left(\frac{V_0}{V}\right)^2 + \frac{3}{4}(1+2\chi)\left(\frac{V_0}{V}\right)^{(4/3)}\right. \\ & \left. - \frac{3}{2}(1+\chi)\left(\frac{V_0}{V}\right)^{(2/3)} + \frac{1}{2}\left(\chi + \frac{3}{2}\right)\right], \end{aligned} \tag{9}$$

[where E_0 and $B_0 = V_0 \frac{d^2E}{dV^2}$ are the values of the energy and bulk modulus at the equilibrium volume V_0, respectively, $\chi = \frac{3}{4}(4 - B_0')$ and $B_0' = (dB_0/dP)$, with derivatives evaluated at zero pressure] and searched iteratively for the f_{att} parameters, which better reproduced the DFT $P_{\text{static}}(V)$ curve obtained with the PBE-vdW functional. Our best fit was attained with $A_{\text{att}} = 0.95$, $R_{\text{att}} = 2.34$ Å, and $C_{\text{att}} = 1.50$, which constitutes our choice of the effective Aziz-M potential.

In Fig. 2, we compare the repulsive core of the original and modified Aziz potentials. Due to the analytical form of function f_{att}, the $V_{\text{Aziz-M}}(r)$ potential displays a positive slope at distances comprised in the interval $0 \leqslant r \leqslant d \sim 1.0$ Å. This feature is manifestly incorrect since it promotes the overlapping of atoms at high densities. Following the strategy explained in Ref. [48], we have corrected for such a flawed behavior by introducing the new potential function

$$V_{\text{Aziz-B}}(r) = V_{\text{Aziz-M}}(r)\Theta(r - R_c) + \tilde{V}_{\text{rep}}(r)\Theta(R_c - r), \tag{10}$$

where $\Theta(x)$ is the Heaviside function, and $\tilde{V}_{\text{rep}}(r)$ a function that is analytically equivalent to V_{rep} but with the two parameters entering its expression adjusted to match the first derivative of $V_{\text{Aziz-M}}(r)$ at $R_c = 1.3$ Å (i.e., $\tilde{\alpha} = 18.745$ and $\tilde{\beta} = 13.143$, to be compared with $\alpha = 10.433$ and $\beta = -2.280$ appearing in the original $V_{\text{rep}}(r)$ factor; see inset in Fig. 2). Function $V_{\text{Aziz-B}}(r)$ with parameters R_c, $\tilde{\alpha}$, and $\tilde{\beta}$, constitute our choice of the effective Aziz-B potential in the remainder of this article. As it is shown in Fig. 2, excellent agreement between the static equations of state calculated with DFT (PBE-vdW) and the Aziz-B potential is obtained.

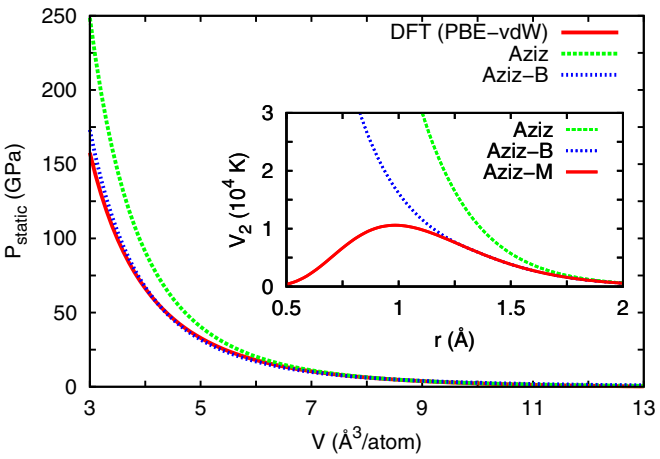

FIG. 2. (Color online) Calculated static equation of state of solid helium (i.e., considering immobile nuclei at the equilibrium lattice positions) using DFT (PBE-vdW) and two effective pairwise interaction models, namely the well-known Aziz potential and the modified version Aziz-B. (Inset) Comparison of the repulsive cores of the Aziz, Aziz-M, and Aziz-B potential models.

D. Diffusion Monte Carlo method

DMC is an accurate computational method that provides the *exact* (i.e., within statistical errors) ground-state energy of a bosonic many-body interacting system [49–51]. The Hamiltonian governing our system is

$$\mathrm{H} = -\frac{\hbar^2}{2m_{\text{He}}}\sum_{i=1}^{N}\nabla_i^2 + \sum_{i<j}^{N} V_2^{\text{eff}}(r_{ij}), \tag{11}$$

where m_{He} is the mass of a ^{4}He atom, r_{ij} the distance between atoms composing a i,j pair, and $V_2^{\text{eff}}(r_{ij})$ a pairwise interatomic model (i.e., V_{Aziz} and $V_{\text{Aziz-B}}$, see Sec. II C). The DMC method is based on a short-time approximation for the Green's function, corresponding to the imaginary time-dependent Schrödinger equation, which is solved up to a certain order of accuracy within an infinitesimal interval $\Delta\tau$. For a detailed description of the DMC technique, we address the interested reader to Refs. [28,49–53].

The guiding wave function used in this work for importance sampling corresponds to the extensively tested Nosanow-Jastrow model [54–56]

$$\psi_{\text{NJ}}(\mathbf{r}_1, \mathbf{r}_2, \ldots, \mathbf{r}_N) = \prod_{i\neq j}^{N} \mathrm{f}_2(r_{ij}) \prod_{i=1}^{N} \mathrm{g}_1(|\mathbf{r}_i - \mathbf{R}_i|), \tag{12}$$

with $\mathrm{f}_2(r) = e^{-\frac{1}{2}(\frac{b}{r})^5}$ and $\mathrm{g}_1(r) = e^{-\frac{1}{2}ar^2}$, and where a and b are variational parameters. This model is composed of two-body correlation functions $\mathrm{f}_2(r)$ deriving from the interatomic potential, and one-body functions $\mathrm{g}_1(r)$ that localize the particles around the positions of the equilibrium lattice $\{\mathbf{R}_i\}$. The Nosanow-Jastrow model is not Bose symmetric under the exchange of particles however ψ_{NJ} has been shown to

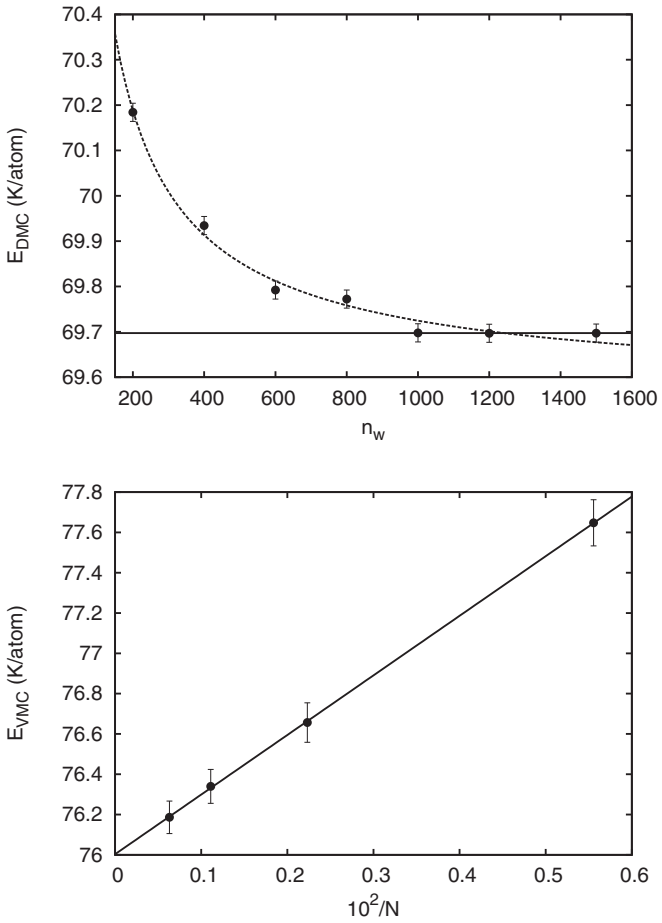

FIG. 3. (a) Dependence of the ground-state energy calculated with the DMC method on the critical population of walkers. The dashed line corresponds to a (monotonically decreasing) inverse power-law fitted to the calculated $E_{\mathrm{DMC}}(n_w)$ energies, whereas the horizontal solid line marks the plateau that is reached at $1000 \leqslant n_w$ values. (b) Dependence of the total energy calculated with the VMC method on the number of particles. Extrapolation to the thermodynamic limit is achieved through a linear fit.

provide very accurate energy and structure results in DMC simulations [57]. We note that the parameters contained in ψ_{NJ} are optimized with the variational Monte Carlo technique (VMC) at each considered density [49]. For instance, at $\rho = 0.06$ Å^{-3}, we obtain $b = 2.94$ Å and $a = 3.21$ Å^{-2}, and at $\rho = 0.33$ Å^{-3}, $b = 1.84$ Å, and $a = 29.08$ Å^{-2}.

Our DMC calculations need to be converged with respect to the time step $\Delta\tau$, critical population of walkers n_w, and number of particles N. We have adjusted $\Delta\tau$ and n_w in order to eliminate any possible bias coming from them. In particular, these are 10^{-4} K^{-1} and 10^3, respectively. In Fig. 3(a), we demonstrate that the selected n_w value perfectly guarantees proper convergence of the total ground-state energy. In fact, we do not observe the monotonically decreasing $1/r$ law reported in Ref. [58] [see Fig. 3(a)]. Finite size errors have been corrected by following the variational approach introduced in Ref. [28], which proved to be very accurate in describing solid ^{4}He at moderate pressures. Namely, the total

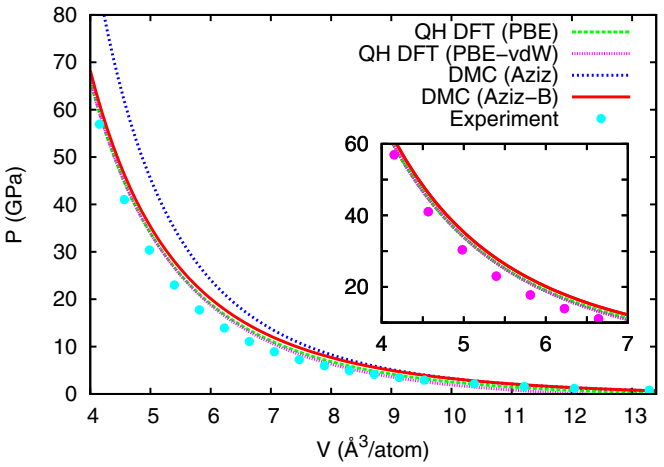

FIG. 4. (Color online) Zero-temperature equation of state of helium calculated with different methods and considering exact (i.e., Aziz and Aziz-B) and approximate (i.e., PBE and PBE-vdW) estimation of quantum nuclear effects. Experimental data found in Ref. [59] are shown for comparison. (Inset) The high-P region in the EOS is zoomed in to appreciate better the differences.

ground-state energy of the system is computed as $E_{\mathrm{DMC}}(\infty) = E_{\mathrm{DMC}}(N_0) + \Delta E^{\mathrm{tail}}_{\mathrm{VMC}}(N_0)$, where

$$\Delta E^{\mathrm{tail}}_{\mathrm{VMC}}(N_0) = E^{\infty}_{\mathrm{VMC}} - E^{N_0}_{\mathrm{VMC}}. \tag{13}$$

In the equation above, energy superscripts indicate the number of particles, $N_0 = 180$ is the number of atoms employed in the DMC simulations, and $E_{\mathrm{VMC}} \equiv \langle\psi_{\mathrm{NJ}}|\mathrm{H}|\psi_{\mathrm{NJ}}\rangle/\langle\psi_{\mathrm{NJ}}|\psi_{\mathrm{NJ}}\rangle$ is the variational energy calculated with the guiding wave function (12). The variational energy in the $N \to \infty$ limit, $E^{\infty}_{\mathrm{VMC}}$, is estimated by successively enlarging the simulation box (i.e., up to 1584 particles) at fixed density and performing a linear extrapolation to infinite volume. Indeed, this procedure turns out to be computationally affordable within VMC but not within DMC. In Fig. 3(b), we show a test case in which the adequacy of the linear extrapolation in $E_{\mathrm{VMC}}(N)$ is demonstrated.

III. RESULTS AND DISCUSSION

In Fig. 4, we show the calculated equation of state (EOS) in solid ^{4}He using (i) DFT and quasiharmonic zero-point energy corrections [i.e., curves PBE and PBE-vdW where $E_{\mathrm{DFT}}(V) = E_{\mathrm{eq}}(V) + E_{\mathrm{harm}}(V)$, see Eqs. (6) and (9)], and (ii) DMC with the effective pairwise potentials V_{Aziz} and $V_{\mathrm{Aziz\text{-}B}}$. For comparison purposes, we include also experimental data from Ref. [59]. Very good agreement is found between experiments and the calculated DMC(Aziz-B) and QH DFT equations of state. In contrast, results obtained with the original Aziz potential and the DMC method largely overestimate the measured pressures (as it was already expected, see Sec. II C). The $P(V)$ curves shown in Fig. 4 are based on the $E(V)$ parametrization introduced in Eq. (9). The optimal parameters obtained in the DMC(Aziz-B) case are $V_0^{\mathrm{DMC}} = 15.92$ Å^3, $B_0^{\mathrm{DMC}} = 2.66$ GPa, and $\chi^{\mathrm{DMC}} = -0.086$; and in the DFT(PBE-vdW) case: $V_0^{\mathrm{DFT}} = 12.23$ Å^3, $B_0^{\mathrm{DFT}} = 6.38$ GPa, and $\chi^{\mathrm{DFT}} = 0.026$ (relative errors associated to these

TABLE I. Energetic and structural properties of dense ^{4}He computed with the DMC method and Aziz-B pairwise model interaction (see text). $N_0 = 180$ and stands for the number of atoms employed in the DMC simulations. Zero-point energies, $E_{\rm harm}$, obtained within the QH DFT approach are enclosed for comparison. Energies are expressed in units of Kelvin and the statistical uncertainties are within parentheses.

V (Å^3)	P (GPa)	B (GPa)	$E_{\rm DMC}$	$\Delta E^{\rm tail}_{\rm VMC}(N_0)$	$E_{\rm kin}$	$E_{\rm harm}$	γ
11.13	2.0 (1)	9.8 (1)	401.8 (1)	−4.2 (1)	174.6 (1)	373 (5)	0.12 (1)
8.35	6.6 (1)	24.1 (1)	1124.8 (1)	−7.9 (1)	265.9 (1)	585 (5)	0.11 (1)
6.68	14.2 (1)	46.7 (1)	2281.1 (1)	−15.8 (1)	347.9 (1)	831 (5)	0.10 (1)
5.57	25.4 (1)	78.6 (1)	3843.9 (1)	−24.2 (1)	419.9 (1)	978 (5)	0.10 (1)
4.77	40.6 (1)	121.6 (1)	5761.7 (1)	−34.3 (1)	479.0 (1)	1132 (5)	0.10 (1)
4.17	60.3 (1)	176.6 (1)	7971.7 (1)	−47.5 (1)	522.1 (1)	1314 (5)	0.10 (1)
3.71	84.8 (1)	243.6 (1)	10413.5 (1)	−64.2 (1)	556.2 (1)	1515 (5)	0.10 (1)
3.34	114.5 (1)	324.9 (1)	13026.6 (1)	−81.7 (1)	567.0 (1)	1714 (5)	0.10 (1)
3.04	149.9 (1)	419.9 (1)	15760.1 (1)	−99.1 (1)	571.9 (1)	1906 (5)	0.10 (1)

quantities typically are 1%–5%). Upon inspection of Fig. 4, one may arrive at the following conclusions: (i) long-range van der Waals interactions are second order in compressed solid ^{4}He thus there is not a real need to consider them in practical simulations, and (ii) quasiharmonic approaches based on DFT appear to be reliable methods for predicting zero-temperature EOS in compressed quantum crystals.

In Fig. 5, we enclose the bulk modulus of ^{4}He, $B(V) = -V(dP/dV)_V$, calculated with the QH DFT and DMC methods (see also Table I). Experimental data from Ref. [60] are also shown for comparison. As in the previous case, we find notable agreement between the DMC(Aziz-B), QH DFT and experimental results, which further demonstrates the reliability of our devised pairwise potential model. We must note here that analysis of the elastic properties in dense helium is beyond the scope of the present work. In fact, it has been known for some time that in order to attain a realistic description of elasticity in rare gases under pressure, it is necessary to consider many-body interactions beyond pairwise [61,62]. We therefore leave the study of these important physical quantities to future work.

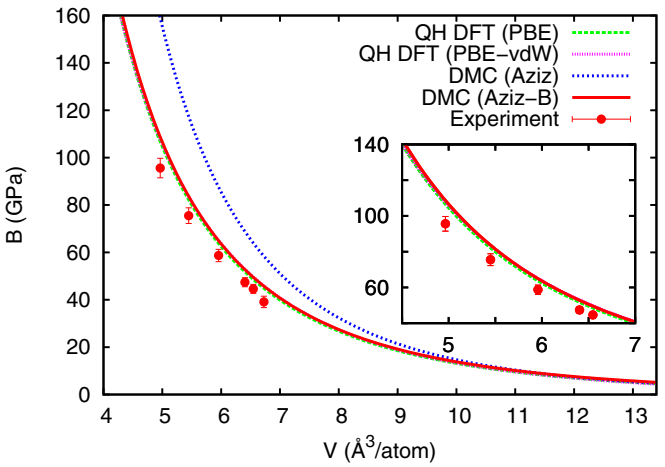

FIG. 5. (Color online) Calculated ^{4}He bulk modulus with different methods and (i.e., Aziz and Aziz-B) and considering approximate (i.e., PBE and PBE-vdW) estimation of quantum nuclear effects. Experimental data found in Ref. [60] are shown for comparison. (Inset) The high-P B region is zoomed in to appreciate better the differences.

As we mentioned in Introduction, the $|E_{\rm kin}/E_{\rm pot}|$ ratio can be regarded as a qualitative indicator of the degree of quantumness of a condensed matter system at $T = 0$ K. Actually, the larger the kinetic energy, the more important quantum nuclear effects are. For instance, in liquid ^{4}He at the equilibrium density, $E_{\rm kin}$ amounts to 14.6 K, which is equal to the ∼67% of the potential energy (in absolute value) [5]. In the quasiharmonic DFT approach, the $|E_{\rm kin}/E_{\rm pot}|$ ratio can be estimated as $|E_{\rm harm}/E_{\rm eq}|$ [see Eq. (6)]. Meanwhile, in the DMC approach, both $E_{\rm pot}$ and $E_{\rm kin} = E - E_{\rm pot}$ energies can be computed exactly (we note that for evaluation of $E_{\rm pot}$, we have employed the pure estimator technique [63,64]) and hence so the $|E_{\rm kin}/E_{\rm pot}|$ ratio. In Fig. 6, we enclose our $|E_{\rm kin}/E_{\rm pot}|$ results obtained with the QH DFT and DMC methods and expressed as a function of pressure (see also Table I). There, it is shown that at pressures below ∼20 GPa ^{4}He behaves as an extreme quantum crystal, wherein the atomic kinetic energy is of the same order of magnitude than the cohesive energy. We also find that the quantum character of solid helium, as

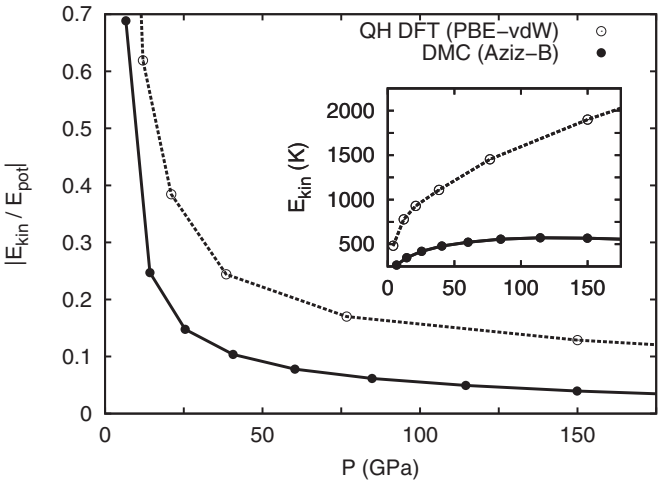

FIG. 6. $|E_{\rm kin}/E_{\rm pot}|$ quantum indicator calculated considering exact (DMC) and approximate (QH DFT) estimation of zero-temperature quantum nuclear effects, expressed as a function of pressure. (Inset) Zero-temperature kinetic energy of solid helium calculated with the DMC and quasiharmonic DFT approaches, expressed as a function of pressure. The dashed and solid lines are guides to the eye.

quantified with the $|E_{kin}/E_{pot}|$ ratio, is progressively depleted with raising pressure. This occurs because the increase in potential energy caused by compression largely surpasses the accompanying increase in the kinetic energy (see Table I). Actually, in Fig. 6, we report the explicit variation of the kinetic energy with pressure: it is found that E_{kin} increases noticeably from equilibrium up to compressions of ∼85 GPa, however, at larger P, it just grows slightly (see Table I). In particular, E_{kin} increases by no more than ∼15 K in the pressure interval $85 \leqslant P \leqslant 150$ GPa. Such a tiny P-induced kinetic energy gain constitutes an original finding, and we will comment again on this in the next paragraphs. Meanwhile, we find that at any conditions the $|E_{kin}/E_{pot}|$ ratio calculated with QH DFT is significantly larger than the values obtained with DMC. In particular, the $E_{harm}(P)$ curve displays always a large positive variation with increasing P, and it lies widely above $E_{kin}(P)$. In fact, kinetic energy discrepancies with respect to the DMC(Aziz-B) results amount to at least ∼50% (see Fig. 6 and Table I). These huge differences indicate that despite QH DFT approaches may provide reasonable EOS (essentially because at high pressures E_{kin} is always small as compared to E_{pot}), these cannot reproduce accurately quantum nuclear effects in dense helium. This conclusion is of fundamental relevance to computational work done in high pressure science, where "zero-point energy" corrections usually turn out to be decisive in the prediction of phase transitions. Namely, according to our analysis QH DFT approaches may fail significantly at determining the $T = 0$ K phase diagram of substances in which quantum nuclear effects are predominant [21,65,66].

The almost flat $E_{kin}(P)$ curve obtained at $P \geqslant 85$ GPa constitutes an original, and to some extent unexpected, finding. Aimed at better understanding the origins of this effect, we computed the ^{4}He Lindemann ratio $\gamma = \sqrt{\langle \mathbf{u}^2 \rangle}/a$ (where the quantity in the numerator represents the averaged mean squared displacement of the atoms taken with respect to their equilibrium hcp positions) as a function of pressure with the DMC and pure estimator techniques [63,64]. The Lindemann ratio results enclosed in Fig. 7 and Table I show that the size of the ^{4}He displacements around their equilibrium positions

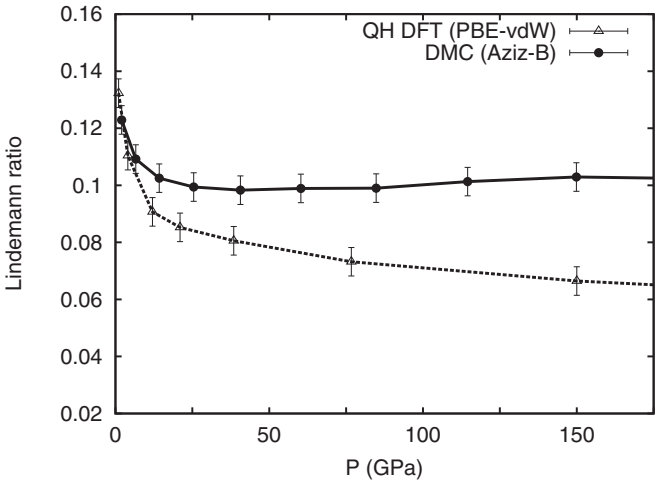

FIG. 7. ^{4}He Lindemann ratio calculated with exact (DMC) and approximate (quasiharmonic DFT) methods, expressed as a function of pressure. The dashed and solid lines are guides to the eye.

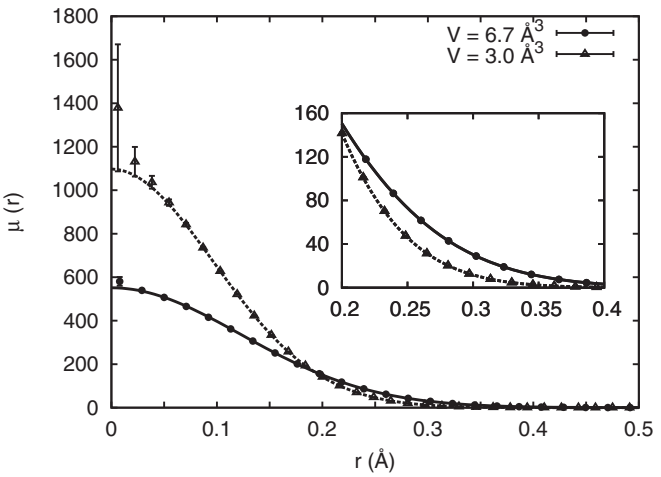

FIG. 8. Radial atomic distribution function calculated with the DMC method and pure estimator technique at $V = 6.7$ and 3.0 Å^3, employing the modified Aziz-B pairwise potential. (Inset) The intermediate region is zoomed in for a better appreciation of the results. Lines correspond to Gaussian fits performed in the displayed r interval.

does not shrink appreciably with compression: γ remains almost constant around 0.10 at $P \geqslant 15$ GPa. This finding is consistent with the already disclosed $E_{kin}(P)$ curve: ^{4}He atoms can persist chiefly delocalized over ample pressure intervals in which their kinetic energy does not increase appreciably as a result of their quantum correlations. Meanwhile, ^{4}He Lindenmann ratios calculated with the QH DFT approach (where $\langle \mathbf{u}^2_{DFT} \rangle$ is estimated as $9\hbar^2/8m_{He}E_{harm}$ [11,67]) exhibit a monotonous decrease with increasing pressure and do not agree with the DMC results obtained at high P (see Fig. 7). These large discrepancies show that structural details in dense quantum solids can neither be described correctly with QH DFT approaches.

In Fig. 8, we report the calculated radial distribution function of ^{4}He atoms, $\mu(r)$, around their equilibrium hcp lattice positions at two different volumes, using the DMC and pure estimator techniques [63,64]. In both cases, it is appreciated that the possibility of finding an atom at a distance larger than ∼0.4 Å from its lattice site is practically zero. As density is increased, the value of the $\mu(r)$ function at the origin increases noticeably whereas the variations on its tail turn out to be less significant (see inset in Fig. 8). This finding is consistent with the γ results explained above and illustrates the high degree of atomic delocalization in dense solid helium. In the same figure, we show Gaussian fits to the $\mu(r)$ results performed in the radial distance interval $r \leqslant 0.5$ Å. It is found that these curves reproduce very well the computed $\mu(r)$ profiles (in fact, reduced chi-square values associated to our data fitting are close to unity). Also, we estimated the kurtosis in the three Cartesian directions (i.e., $\zeta = \langle \mathbf{u}^4 \rangle / \langle \mathbf{u}^2 \rangle^2 - 3$) [11] and found values compatible with zero in all the cases (i.e., $0.01 - 0.001$).

Finally, in Fig. 9, we enclose the radial pair distribution function calculated in dense ^{4}He, considering both the Aziz-B and Aziz interaction models, with the DMC and pure estimator techniques [63,64]. It is observed that the ground-state system rendered by the Aziz-B interaction is less structured than

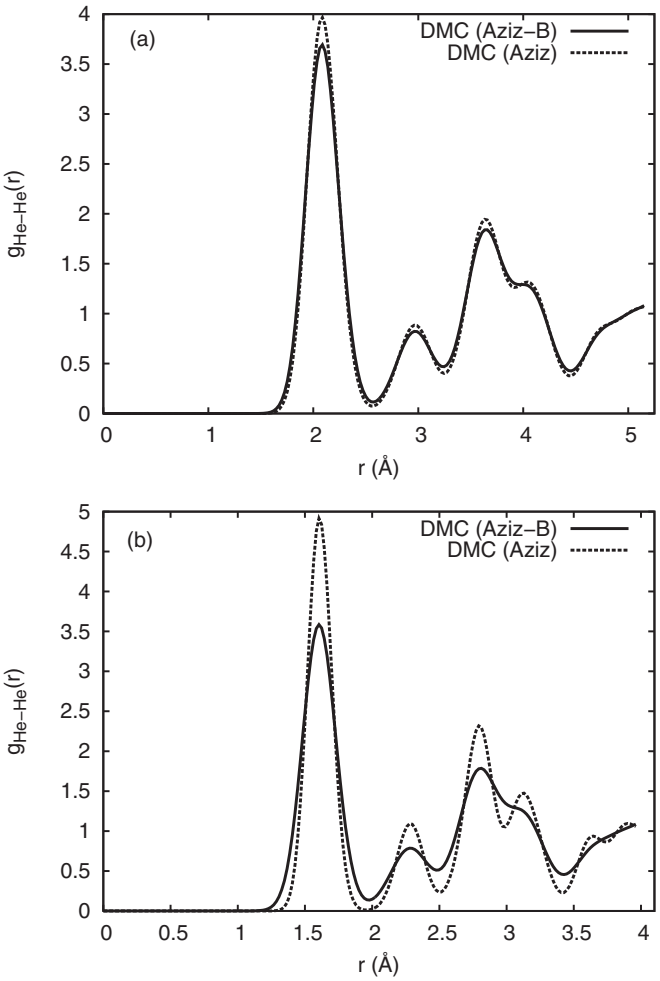

FIG. 9. Radial pair distribution function calculated with the DMC method and pure estimator techniques at volumes (a) $V = 6.7$ and (b) 3.0 Å^3, employing the original and modified Aziz pairwise potentials.

the one obtained with the original Aziz potential, due to its softer core. The position of the $g(r)$ maxima, however, roughly appear at the same distances in both cases.

IV. CONCLUSIONS

We have performed a computational study of the quantum nuclear effects in compressed ^{4}He at zero temperature by relying exclusively on first-principles methods. For the description of the electronic degrees of freedom, we employ a nonstandard implementation of density functional theory (DFT) which is able to deal efficiently with long-range van der Waals interactions. For the simulation of quantum nuclear effects, we employ the diffusion Monte Carlo method and a modified version of the pairwise Aziz potential, Aziz-B, that closely reproduces the static compression curve obtained with DFT. The Aziz-B potential is softer than Aziz one at short distances in a way that is rather similar to the behavior observed in molecular hydrogen [20,48]. This softening of the potential wall is an effective pairwise approximation to many-body interaction terms which, according to our DFT results, are predominantly attractive [68]. In fact, the Aziz-B interaction model introduced in this work may be used by others for the simulation of solid ^{4}He at high pressures and low temperatures. We find that when solid helium is compressed, the resulting gain in potential energy largely surpasses the accompanying increase in the kinetic energy. In particular, we show that the kinetic energy of ^{4}He atoms increases very slightly under compression at pressures larger than ∼85 GPa. Also, we find that the Lindemann ratio in dense solid helium amounts to 0.10 almost independently of pressure. These results evidence the presence of strong quantum correlations in compressed ^{4}He crystals, which allow the atoms to remain remarkably delocalized over a wide range of pressures. In addition to this, we perform analogous calculations using the quasiharmonic DFT approach. We find that this method, which customarily is employed in computational high-P studies, cannot reproduce with reliability the kinetic energy and structural traits of compressed ^{4}He at zero temperature. In particular, the kinetic energy discrepancies found with respect to the full quantum calculations amount to at least 50%. The conclusions presented in this work are of critical importance for modeling of light and weakly interacting materials (e.g., H_2, CH_4, and NH_3) done in high-pressure studies and related to Earth and planetary sciences.

ACKNOWLEDGMENTS

This research was supported under the Australian Research Council's Future Fellowship funding scheme (Project No. RG134363), MICINN-Spain (Grants No. MAT2010-18113, No. CSD2007-00041, and No. FIS2011-25275), and Generalitat de Catalunya (Grant No. 2009SGR-1003).

[1] L. K. Moleko and H. R. Glyde, Phys. Rev. Lett. **54**, 901 (1985).
[2] S. O. Diallo, J. V. Pearce, R. T. Azuah, and H. R. Glyde, Phys. Rev. Lett. **93**, 075301 (2004).
[3] C. A. Burns and E. D. Isaacs, Phys. Rev. B **55**, 5767 (1997).
[4] R. A. Aziz, F. R. W. McCourt, and C. C. K. Wong, Mol. Phys. **61**, 1487 (1987).
[5] J. Boronat and J. Casulleras, Phys. Rev. B **49**, 8920 (1994).
[6] D. M. Ceperley, Rev. Mod. Phys. **67**, 279 (1995).
[7] D. M. Ceperley and B. J. Alder, Phys. Rev. B **36**, 2092 (1987).
[8] C. Cazorla and J. Boronat, Phys. Rev. B **78**, 134509 (2008).
[9] J. Boronat, C. Cazorla, D. Colognesi, and M. Zoppi, Phys. Rev. B **69**, 174302 (2004).
[10] C. Cazorla and J. Boronat, J. Low Temp. Phys. **139**, 645 (2005).
[11] C. Cazorla and J. Boronat, Phys. Rev. B **77**, 024310 (2008).
[12] C. Cazorla and J. Íñiguez, Phys. Rev. B **88**, 214430 (2013).
[13] S. A. Shevlin, C. Cazorla, and Z. X. Guo, J. Phys. Chem. C **116**, 13488 (2012).

[14] C. Cazorla, D. Alfè, and M. J. Gillan, Phys. Rev. B **85**, 064113 (2012).
[15] C. Cazorla and D. Errandonea, Phys. Rev. B **81**, 104108 (2010).
[16] C. Cazorla, D. Errandonea, and E. Sola, Phys. Rev. B **80**, 064105 (2009).
[17] Yu. A. Freiman, S. M. Tretyak, A. Grechnev, A. F. Goncharov, J. S. Tse, D. Errandonea, H. K. Mao, and R. J. Hemley, Phys. Rev. B **80**, 094112 (2009).
[18] Yu. A. Freiman, A. Grechnev, S. M. Tretyak, A. F. Goncharov, and R. J. Hemley, Phys. Rev. B **86**, 014111 (2012).
[19] Yu. A. Freiman, A. Grechnev, S. M. Tretyak, A. F. Goncharov, C. S. Zha, and R. J. Hemley, Phys. Rev. B **88**, 214501 (2013).
[20] M. Moraldi, J. Low Temp. Phys. **168**, 275 (2012).
[21] G. Geneste, M. Torrent, F. Bottin, and P. Loubeyre, Phys. Rev. Lett. **109**, 155303 (2012).
[22] G. Gao *et al.*, J. Chem. Phys. **133**, 144508 (2010).
[23] P. Loubeyre *et al.*, Nature (London) **383**, 702 (1996).
[24] J. M. McMahon, M. A. Morales, C. Pierleoni, and D. M. Ceperley, Rev. Mod. Phys. **84**, 1607 (2012).
[25] C. J. Pickard and R. J. Needs, Nat. Mater. **7**, 775 (2008).
[26] R. M. Martin, *Electronic Structure* (Cambridge University Press, Cambridge, 2004).
[27] J. Kohanoff, *Electronic Structure Calculations for Solids and Molecules: Theory and Computational Methods* (Cambridge University Press, Cambridge, 2006).
[28] C. Cazorla and J. Boronat, J. Phys.: Condens. Matter **20**, 015223 (2008).
[29] M. J. Gillan, D. Alfè, J. Brodholt, L. Vočadlo, and G. D. Price, Rep. Prog. Phys. **69**, 2365 (2006).
[30] C. Cazorla, D. Alfè, and M. J. Gillan, Phys. Rev. B **77**, 224103 (2008).
[31] M. Dion, H. Rydberg, E. Schröder, D. C. Langreth, and B. I. Lundqvist, Phys. Rev. Lett. **92**, 246401 (2004).
[32] M. A. Basanta, Y. J. Dappe, J. Ortega, and F. Flores, Europhys. Lett. **70**, 355 (2005).
[33] N. D. Drummond and R. J. Needs, Phys. Rev. B **73**, 024107 (2006).
[34] Z. Nabi, L. Vitos, B. Johansson, and R. Ahuja, Phys. Rev. B **72**, 172102 (2005).
[35] J. P. Perdew, K. Burke, and M. Ernzerhof, Phys. Rev. Lett. **77**, 3865 (1996).
[36] S. Grimme, J. Comp. Chem. **27**, 1787 (2006).
[37] P. E. Blöchl, Phys. Rev. B **50**, 17953 (1994).
[38] G. Kresse and D. Joubert, Phys. Rev. B **59**, 1758 (1999).
[39] G. Kresse and J. Furthmüller, Phys. Rev. B **54**, 11169 (1996).
[40] C. Cazorla, M. J. Gillan, S. Taioli, and D. Alfè, J. Chem. Phys. **126**, 194502 (2007).
[41] S. Taioli, C. Cazorla, M. J. Gillan, and D. Alfè, Phys. Rev. B **75**, 214103 (2007).
[42] C. Cazorla, D. Alfè, and M. J. Gillan, Phys. Rev. Lett. **101**, 049601 (2008).
[43] G. Kresse, J. Furthmüller, and J. Hafner, Europhys. Lett. **32**, 729 (1995).
[44] D. Alfè, G. D. Price, and M. J. Gillan, Phys. Rev B **64**, 045123 (2001).
[45] D. Alfè, Comp. Phys. Commun. **180**, 2622 (2009).
[46] H. J. Monkhorst and J. D. Pack, Phys. Rev. B **13**, 5188 (1976).
[47] F. Birch, J. Geophys. Res. **83**, 1257 (1978).
[48] T. Omiyinka and M. Boninsegni, Phys. Rev. B **88**, 024112 (2013).
[49] B. L. Hammond, W. A. Lester Jr., and P. J. Reynolds, *Monte Carlo Methods in Ab initio Quantum Chemistry* (World Scientific, Singapore, 1994).
[50] R. Guardiola, in *Microscopic Quantum Many-Body Theories and Their Applications*, edited by J. Navarro and A. Polls (Springer, Berlin, 1998).
[51] D. M. Ceperley and M. H. Kalos, *Monte Carlo Methods in Statistical Physics* (Springer, Berlin, 1979).
[52] M. H. Kalos, D. Levesque, and L. Verlet, Phys. Rev. A **9**, 2178 (1974).
[53] S. A. Chin, Phys. Rev. A **42**, 6991 (1990).
[54] L. H. Nosanow, Phys. Rev. Lett. **13**, 270 (1964).
[55] J. P. Hansen and D. Levesque, Phys. Rev. **165**, 293 (1968).
[56] J. P. Hansen, Phys. Lett. A **30**, 214 (1969).
[57] C. Cazorla, G. Astrakharchick, J. Casulleras, and J. Boronat, New J. Phys. **11**, 013047 (2009).
[58] M. Boninsegni and S. Moroni, Phys. Rev. E **86**, 056712 (2012).
[59] P. Loubeyre, R. LeToullec, J. P. Pinceaux, H. K. Mao, J. Hu, and R. J. Hemley, Phys. Rev. Lett. **71**, 2272 (1993).
[60] C.-S. Zha, H.-K. Mao, and R. J. Hemley, Phys. Rev. B **70**, 174107 (2004).
[61] E. Pechenik, I. Kelson, and G. Makov, Phys. Rev. B **78**, 134109 (2008).
[62] M. Grimsditch, P. Loubeyre, and A. Polian, Phys. Rev. B **33**, 7192 (1986).
[63] R. Barnett, P. Reynolds, and W. A. Lester Jr., J. Comput. Phys. **96**, 258 (1991).
[64] J. Casulleras and J. Boronat, Phys. Rev. B **52**, 3654 (1995).
[65] S. Biermann, D. Hohl, and D. Marx, Solid State Commun. **108**, 337 (1998).
[66] H. Kitamura, H. Kitamura, T. Ogitsu, and T. Miyake, Nature (London) **404**, 259 (2000).
[67] D. A. Arms, R. S. Shah, and R. O. Simmons, Phys. Rev. B **67**, 094303 (2003).
[68] P. Loubeyre, Phys. Rev. Lett. **58**, 1857 (1987).